Measurement of Brown Adipose Tissue Mass using a Novel Dual-Echo Magnetic Resonance Imaging Approach: A Validation Study.

Milja Holstila, MD[a], Kirsi A. Virtanen, MD, PhD [b], Tove J. Grönroos, MSc, PhD[b], Jukka Laine, MD, PhD[c], Virva Lepomäki, MSc[b], Jani Saunavaara MSc, PhD[a], Irina Lisinen, MSc[b], Markku Komu, MSc, PhD[a], Jarna C. Hannukainen[b], MSc, PhD, Pirjo Nuutila, MD, PhD[b,d], Riitta Parkkola, MD, PhD[a], Ronald J.H. Borra, MD, PhD[a,b,e]

[a]Medical Imaging Centre of Southwest Finland, Turku University Hospital, Turku, Finland

[b]Turku PET Centre, University of Turku and Turku University Hospital, Turku, Finland

[c]Department of Pathology, University of Turku and Turku University Hospital, Turku, Finland

[d]Department of Medicine, University of Turku and Turku University Hospital, Turku, Finland

[e]A. A. Martinos Center for Biomedical Imaging, Massachusetts General Hospital, Boston, MA, USA

Correspondence:

Riitta Parkkola, MD, PhD, Medical Imaging Centre of Southwest Finland

Turku University Hospital, P.O. Box 52, FI-20521 Turku, Finland

email: riitta.parkkola@tyks.fi

Phone: +358 2 313 0148, Fax: +358 2 313 2950

Word count of text: 3645

Word count of abstract: 248

Number of references: 31

Number of tables: 1

Number of figures: 6

Disclosure statement:

This study was conducted within the Finnish Centre of Excellence in Molecular Imaging in Cardiovascular and Metabolic Research, which is supported by the Academy of Finland, University of Turku, Turku University Hospital and Åbo Akademi University. Additionally, RJHB received personal research grants from the Sigrid Juselius Foundation, the Instrumentarium Research Foundation, the Academy of Finland, the Paulo Foundation and the Finnish Medical Foundation. There are no potential conflicts of interest related to this article.

Abstract

Objective: The aim of this study was to evaluate and validate magnetic resonance imaging (MRI) for the visualization and quantification of brown adipose tissue (BAT) *in vivo* in a rat model. We hypothesized that, based on differences in tissue water and lipid content, MRI could reliably differentiate between BAT and white adipose tissue (WAT) and could therefore be a possible alternative for ^{18}F-Fluorodeoxyglucose Positron Emission Tomography (^{18}FDG-PET), the current gold standard for non-invasive BAT quantification.

Materials/Methods: Eleven rats were studied using both ^{18}FDG-PET/CT and MRI (1.5 T). A dual echo (in-and-out-of-phase) sequence was used, both with and without spectral presaturation inversion recovery (SPIR) fat suppression (DUAL-SPIR) to visualize BAT, after which all BAT was surgically excised. The BAT volume measurements obtained via ^{18}FDG-PET/CT and DUAL-SPIR MR were quantitatively compared with the histological findings. All study protocols were reviewed and approved by the local ethics committee.

Results: The BAT mass measurements that were obtained using DUAL-SPIR MR subtraction images correlated better with the histological findings (P=0.017, R=0.89) than did the measurements obtained using ^{18}FDG-PET/CT (P=0.78, R=0.15), regardless of the BAT metabolic activation state. Additionally, the basic feasibility of the DUAL-SPIR method was demonstrated in three human pilot subjects.

Conclusions: This study demonstrates the potential for MRI to reliably detect and quantify BAT in vivo. MRI can provide information beyond that provided by ^{18}FDG-PET imaging,

and its ability to detect BAT is independent of its metabolic activation state. Additionally, MRI is a low-cost alternative that does not require radiation.

Key words: Cold Exposure, ^{18}FDG-PET, Rat

List of abbreviations: MRI = magnetic resonance imaging, BAT = brown adipose tissue, WAT = white adipose tissue, ^{18}FDG-PET = ^{18}F-Fluorodeoxyglucose positron emission tomography, CT = computed tomography, FDG = fluorodeoxyglucose, SPIR = spectral presaturation inversion recovery

Introduction

Background

Two types of adipose tissue are present in the human body: brown and white adipose tissue. The predominant adipose tissue type, white adipose tissue (WAT), is the primary site of regular energy storage, whereas the thermogenic metabolic activity of brown adipose tissue (BAT), which is innervated by the sympathetic nervous system, is more acutely induced by dieting and cold temperatures [1, 2]. Long-term cold exposure is believed to increase the volume of BAT [3-5], while short-term cold exposure causes metabolic activation [1, 6]. The important role of BAT, as determined by in vivo study, in cold-induced thermogenesis in human adult energy balance has attracted tremendous interest recently, especially because changes in BAT may have a role in the pathogenesis of type 2 diabetes and obesity [7-9].

BAT has been reported to account for 11.8% of the resting metabolic rate, albeit with high individual variation [10]. The amount of brown adipose tissue is inversely correlated with body-mass index, which strongly suggests that brown adipose tissue may have a role in adult human metabolism [2, 11]. Additionally, outside temperature, sex, body mass index and diabetic status have all been shown to affect the glucose-uptake activity of BAT in humans [12, 13].

To date, in vivo observations of BAT have been performed mainly using clinical ^{18}F-fluorodeoxyglucose positron emission tomography (^{18}FDG-PET); these observations have revealed that a substantial fraction of adult humans have areas of symmetrical high FDG uptake [14]. In adult humans, the most common location for BAT is the cervical–supraclavicular depot [11]. BAT can also be found in paravertebral, mediastinal, para-aortic, and suprarenal locations [11, 12]. However, the visibility of subclavicular depots of BAT by

^{18}FDG-PET in humans has been validated by biopsies only recently [1]. In studies conducted after cold exposure, the prevalence of detectable BAT depots by ^{18}FDG-PET approaches 100% in healthy volunteers [6].

In clinical settings, MRI has been considered the most suitable modality for imaging and quantifying fat tissue due to its superior soft-tissue contrast and resolution. Some studies of BAT-containing tumors, such as pheochromocytomas [15] and hibernomas [16-19], have been reported, but none of them characterized BAT using MRI in healthy humans. In rats, several MR techniques, including magnetic spectroscopy [23,24], have been employed to quantify BAT using 4.7 T, 7 T and 9.4 T small bore animal MR systems [20-23]. The most promising approach seems to be in- and out-of-phase imaging [21, 22, 25]. Additionally, fat water mapping at a field strength of 3 T has been used to quantify BAT in mice [26].

These techniques are based on the fact that brown adipose tissue has a higher water content than WAT, which should allow the differentiation of BAT from the surrounding WAT tissue using in- and out-of-phase imaging [28]. Furthermore, while ^{18}FDG-PET/CT only identifies activated BAT that has increased metabolic activity (glucose uptake), MRI provides superior anatomical resolution and thus has the potential to determine BAT volume in a more reliable fashion, regardless of the activation state. To the best of our knowledge, no studies comparing MR in- and out-of-phase imaging with ^{18}FDG-PET and histology have been previously reported.

Rationale

In the current study, we aimed to validate our novel and rapid method of BAT imaging at 1.5 Tesla magnetic field strength using in- and out-of-phase dual echo MR imaging combined

with spectral presaturation inversion recovery (DUAL-SPIR) in a rat model by directly comparing the MR findings with those of ^{18}FDG-PET/CT and histology. Additionally, we aimed to demonstrate the feasibility of this technique for detecting BAT in the cervical–supraclavicular region of a healthy human subject.

Methods

Ethical approval

The animal study protocol was reviewed by Ethics Committee for Animal Experimentation at the University of Turku, Finland and was approved by the State Provincial Office of Western Finland (STH39A//ESLH-2006-11128/Ym-23).

Study animals and design

Eleven male Sprague-Dawley rats, weighing 325-400 g, bred at the animal facility of the University of Turku were housed under standard conditions (20 ± 1 °C, humidity 55 ± 5%, lights on from 6:00 a.m. to 6:00 p.m.) with free access to standard food and tap water. Because our local Ethics Committee did not grant permission for cold exposure of the rats, they were not exposed to cold. On a given study day, an ^{18}FDG-PET/CT scan was performed first and was then followed by an MR study. The animals were anaesthetized via isoflurane inhalation during the ^{18}FDG-PET/CT scan and then euthanized by CO_2-gas prior to the MR studies. After the MR scan, the BAT tissue of the rats was located visually through careful dissection, and it was then removed and weighed. The removed BAT tissue was also immunohistochemically stained and analyzed. All of the rats were euthanized approximately 5 hours prior to the BAT dissection and histological analysis.

^{18}FDG-PET/CT studies

^{18}FDG-PET/CT scans were performed on eight rats using a hybrid PET/CT animal scanner, Siemens Inveon PET/CT (Siemens Medical Solutions, Knoxville, USA). ^{18}FDG (16.45±0.64 MBq) was injected via a cannula inserted in the tail vein. The rats were anaesthetized with isoflurane 60 min prior to a 20-min static PET scan that was preceded by a low-resolution CT scan used for attenuation correction and anatomical reference. The body temperature was not actively influenced or regulated during neither the 60-min biodistribution period of ^{18}FDG nor the PET/CT scan. The images were reconstructed using an OSEM2D algorithm, and ROIs were drawn on the expected BAT tissue, WAT tissue, and heart muscle using the areas with high ^{18}FDG uptake and/or the CT anatomical reference scan. The ^{18}FDG uptake of the tissues was quantitatively evaluated by comparing the uptake of the interscapular BAT deposits with the heart muscle and subcutaneous white adipose tissue. The volume of the metabolically activated BAT in the ^{18}FDG-PET images was measured using the Mirada 7D software package on the PET/CT workstation (Mirada Solutions Ltd., Oxford, England). The PET scans were analyzed independently, and the reader (TJG) was blinded to all other information.

In-and-out-of-phase MR imaging

Imaging was performed on a Philips Gyroscan Intera CV Nova Dual 1.5 T MRI scanner (Philips Medical Systems, the Netherlands). A circular C3 surface coil was used as the receiving coil. The standard dual gradient echo (in phase – opposite phase) sequence was used with a repetition time (TR) of 10.1 ms, echo times (TE) of 2.30 ms and 4.60 ms, flip angle (FA) of 80° and two averages. The acquisition matrix was 240x240 with foldover suppression, the field of view (FOV) was 140 mm, and the slice thickness was 0.5 mm with a 0.1 mm gap between adjacent slices. In total, 70 sagittal and 70 axial slices of the interscapular area were obtained. The MR analysis was performed independently, and the reader (MH) was blinded to all other information at the time of analysis.

DUAL-SPIR MR imaging

In addition to the basic imaging protocol, we enhanced our imaging technique by combining the in- and out-of-phase series described above with a spectral presaturation inversion recovery (SPIR) pulse, which preceded the dual-echo acquisition, a method we referred to DUAL-SPIR. The inversion pulse [29] was adjusted such that the zero crossing of the T1 relaxation of the lipid signal occurred at the center of the excitation pulse. During the multi-slice scans, a fat suppression pulse was applied before every slice. These DUAL-SPIR images were obtained from six rats, and all of the other parameters, except for the addition of the SPIR pulse, were identical to the conventional in- and out-of-phase imaging series described above.

Image data post-processing

The MRI images were post-processed by subtracting the out-of-phase images from the in-phase images within both the series of conventional in- and out-of-phase data and the DUAL-SPIR data. Post-processing was performed on a Siemens Leonardo workstation (syngo MMWP VE27A, Siemens AG, Berlin and Munchen). Brown adipose tissue, as defined by the remaining bright interscapular signal intensity in each subtraction series, was outlined in each consecutive slice using a freehand ROI tool. The outlined tissue volume was calculated offline by multiplying the outlined areas with the slice thickness, also taking into account the interslice gap. The MR images, the originals and the images obtained from the subtraction series, were also fused with the PET images to facilitate a more direct comparison between the two modalities. This fusion was accomplished using the Mirada 7D software package on a PET/CT workstation (Mirada Solutions Ltd., Oxford, England). Through co-registration of the anatomical MRI and CT data and application of the same transfer matrix to the PET data

and the acquired subtraction MRI data, highly accurate fusion of the MR and PET data were obtained. A 3D-reconstruction video illustrating the final fusion of the DUAL-SPIR MR data with the ^{18}FDG-PET data is available in the online supplementary material. Measured tissue volumes were converted to weights assuming an average BAT tissue density of 0.94 g/cm^3.

Human pilot subjects

The human protocol was reviewed and approved by the Ethics Committee of the Hospital District of Southwest Finland, and written informed consent was obtained from the subjects. The study conformed to the standards set by the latest revision of the Declaration of Helsinki. Three human subjects, one healthy male and two healthy females of normal weight, were exposed to cold conditions prior to ^{18}FDG-PET/CT as previously described [1]. The purpose of the cold exposure was to metabolically activate BAT [2,5]. The MR examination was performed at a later time under normal warm conditions. The imaging parameters were virtually identical to those used in the animal studies: field-of-view (FOV), 530 mm; acquisition matrix, 256x179; slice thickness, 4 mm with a 4 mm gap between adjacent slices; repetition time (TR), 120 ms; echo time (TE), 2.30 ms and 4.60 ms; and flip angle (FA), 80° and one average. A number of slices covering the entire cervical–supraclavicular region were selected and were obtained both with and without the presence of a spectral presaturation inversion recovery (SPIR) pulse.

Histology

As mentioned previously, all visible BAT was carefully dissected in all eleven rats. Immediately upon dissection, the brown adipose tissue was immersed and fixed in 10% buffered formalin (pH 7.4) and subsequently embedded in paraffin. Five-micrometer sections were cut and stained with hematoxylin and eosin. The histological criteria for the tissue to be

labeled as brown fat were the following: dense capillary vasculature; typical multiple small vesicles in the cytoplasm; and strong eosinophilic cytoplasmic staining (rather than a single fat droplet observed in the white adipose tissue cells). Using both morphological and immunohistochemical methods, more than 90% of the dissected tissue was confirmed to be BAT. The remaining tissue was composed of small amounts of fibro-fatty tissue, vessels and muscle.

Statistical methods

All statistical analyses were performed by an experienced biostatistician (IL). Comparisons between the measurement techniques were performed using a paired t-test. The relationship between BAT obtained through the autopsy and imaging methods was calculated using Pearson's correlation. Agreement between the BAT mass acquired by different imaging techniques and the mass acquired by histology was assessed using Bland-Altman plots. All tests were performed with SAS version 9.2 (SAS Institute Inc., Cary, NC). P values <0.05 were considered statistically significant.

Results

Visualization of BAT using MRI

In both the conventional in- and out-of-phase and DUAL-SPIR MRI series, BAT appeared as an area with high signal intensity compared to the background signal intensity (Figure 1). The subtraction images both enhanced the areas with high signal intensity and reduced all other (non-BAT) signal intensities in the image, thus greatly facilitating the differentiation of BAT from WAT (Figure 1A and 1B). In conventional in- and out-of-phase series, the skin and subcutaneous tissues had signal intensities close to those of BAT, thus confounding the identification of BAT. However, this problem was eliminated in the DUAL-SPIR subtraction imaging series (Figure 1C).

Comparison of ^{18}FDG-PET/CT and MRI

The fused ^{18}FDG-PET/MRI data allowed visualization of both the functional BAT on ^{18}FDG-PET and the anatomy of BAT on MRI. In three animals, there was no clear metabolic activation of BAT as determined by ^{18}FDG-PET imaging. The majority of the ^{18}FDG-PET uptake was observed within the large dorsal fat depot in the interscapular area, and lower uptake was observed in the dorsal cervical area (Figure 2 and 3). The interscapular BAT was roughly butterfly shaped, with lateral wings and a central body extending to the neck area. The volume of activated BAT as measured from ^{18}FDG-PET/CT was significantly smaller than the volume of the anatomical area of BAT in the MR images (0.05 mm^3 versus 0.19 mm^3 (P=0.0016), respectively).

Comparison of histological and imaging findings

The BAT tissue masses obtained through dissection were comparable with the BAT masses calculated from the MRI and PET data, (Table 1), although some of the data from all of the

modalities were unavailable in each animal due to technical difficulties. The BAT mass measured from the DUAL-SPIR subtraction images showed the best correlation and best agreement, according to the Bland-Altman analysis, with the dissected BAT mass (P=0.017, R=0.89, Figure 4 and 5).

Human pilot cases

In the 3 healthy human volunteers, both the conventional in- and out-of-phase data and the DUAL-SPIR MR data showed BAT as bright tissue on a darker background (Figure 6A), in agreement with the findings observed in the animal experiments. Metabolic activation of BAT was clearly visible by ^{18}FDG-PET/CT examination (Figure 6B), with bilateral areas of high ^{18}FDG uptake in the cervical–supraclavicular region. Excellent visual correspondence between the metabolically active BAT areas on ^{18}FDG-PET/CT and the areas associated with BAT depots on DUAL-SPIR MRI was observed, as indicated by the direct fusion of the ^{18}FDG-PET and MRI images (Figure 6C). Case 1 had 51 g of brown adipose tissue as measured by DUAL-SPIR MRI and 54 g as measured by ^{18}FDG-PET/CT. For cases 2 and 3, the amount of BAT measured with DUAL-SPIR MRI versus ^{18}FDG-PET/CT, was 32 g versus and 46 g and 53 g versus 16 g, respectively.

Discussion

Interpretation

In this study, we demonstrated and validated the imaging of brown adipose tissue (BAT) in vivo using a clinical 1.5 T MRI scanner. We showed that, using both histology and ^{18}FDG-PET as methods of reference, BAT can be visualized with both conventional in- and out-of-phase imaging and our novel DUAL-SPIR method. However, in our study, only DUAL-SPIR subtraction images allowed unequivocal definition of BAT deposits. In addition, the mass of the BAT deposits measured using the DUAL-SPIR method correlated best with the histological findings. The brown adipose tissue masses calculated from ^{18}FDG-PET/CT were considerably smaller than both the BAT masses obtained through dissection and those obtained with the DUAL-SPIR method. Furthermore, conventional in- and out-of-phase imaging tended to slightly overestimate the amount of BAT. These data strongly suggest that the determination of BAT mass in vivo using DUAL-SPIR MRI is more accurate than PET, the current standard for the non-invasive detection of BAT. We suggest that this effect is caused by the ability of DUAL-SPIR MRI to detect BAT regardless of its metabolic activation state. Based on the data obtained in the current study, we suggest that DUAL-SPIR MR is an appealing alternative for ^{18}FDG-PET in the imaging of BAT depots, as it eliminates the need for ionizing radiation and subject cold exposure.

Our feasibility study confirmed the presence and location of BAT, which were consistent with previous findings obtained using high-field animal MRI [20-22] at 3 T [26,27] and ^{18}FDG-PET/CT scans. Our proposed method allowed the visualization of interscapular BAT deposits in rats, as well as the delineation of tissue areas consisting of fat with markedly higher water content compared to ordinary white adipose tissue (WAT). In the post-processed images acquired by subtracting the out-of-phase images from the in-phase images, BAT was clearly

visualized as bright tissue on darker background, as expected from the relatively higher water content of BAT compared to WAT. Additionally, the proposed method seemed to work well in a single human subject, indicating that there is potential for visualizing BAT using MR in humans.

Strengths and weaknesses

Our study is mainly limited by the relatively small number of animals, as well as various practical limitations that resulted in some of the examinations being unavailable in each animal. In total, this study involved eleven rats; ^{18}FDG-PET/CT and DUAL-SPIR MRI imaging were performed in eight and six animals, respectively. Furthermore, the animals could not be exposed to cold because of ethical considerations, which makes the extrapolation and comparison with human studies more challenging, as the proper cold exposure in human studies might have resulted in higher metabolic activation of BAT on ^{18}FDG-PET/CT.

Additionally, we are aware that our in- and out-of-phase based DUAL-SPIR method does not take into account individual peaks of the lipid spectrum and their individual T1 relaxation behavior, are the overall tissue T2* relaxation effects taken into account either [30,31]. However, we feel that this limitation is out weighed by the fact that the standard in-phase and out-of-phase sequence used to generate our data is available to most MR professionals, and therefore does not limit the reproducibility of our proposed method to the owners of devices from a specific vendor. Our data show that, despite the admittedly simplified imaging and post-processing methods, it is possible to non-invasively identify BAT using this approach.

We recognize that in human subjects the technical challenges are even bigger than in rats, in particular because of the larger and more irregular shape of the imaged cervical area. These

anatomical constraints combined with the technical limitations of modern MR-scanners in terms of maximum magnetic field homogeneity (shimming) can cause imaging artefacts in some subjects. For these reasons we are currently still in the process of optimizing and validating the technique for use in humans.

Implications

The healthy volunteers in this study provide examples of how the technique can be used in human subjects. We will continue our efforts regarding the application this technique to human subjects and patients in the future. In human subjects, the technical aspects of this method are more demanding than in rats because of the larger size and irregular shape of the imaged area. These complications can also lead to challenges in shimming the magnetic field, which can in turn produce artifacts in certain subjects. Therefore, we will need to optimize and validate this technique in humans separately using PET and/or histological samples as the gold standard.

Given the benefits of MRI over ^{18}FDG-PET/CT in animal studies, we foresee that BAT quantification using MRI might facilitate studies in humans due to its wider availability, lack of ionizing radiation and a shorter pre-examination preparation times (because cold exposure for the metabolic activation of BAT is not needed). MRI could also be used as a complementary method to ^{18}FDG-PET/CT, with MRI providing additional information to the ^{18}FDG-PET/CT data by means of its superior anatomical resolution and soft tissue contrast. Additionally, the proposed method could be highly interesting in the light of the rapidly expanding research field of whole-body (hybrid) MR-PET, potentially allowing for detailed simultaneous evaluation of overall and metabolically activated BAT masses in humans.

Conclusion

The present study demonstrates that brown adipose tissue (BAT) can be detected and accurately quantified in vivo using dedicated DUAL-SPIR MRI, regardless of the BAT metabolic activation state. The proposed method offers clear benefits over ^{18}FDG-PET/CT, the current gold standard for non-invasive BAT quantification; these advantages include more accurate quantification, a lack of ionizing radiation and the avoidance of subject cold exposure. We speculate that the use of this (widely available) MR-based technique has the potential to aid future studies on the thus far largely unknown role of BAT, in both healthy and diseased states. This information, in turn, is expected to be essential for future research into energy balance dynamics, potentially leading to new clinical applications for the prevention and treatment of obesity and related pathophysiology.

Author's Translational perspective

MRI provides information beyond that offered by ^{18}FDG-PET imaging due to its ability to detect and quantify brown adipose tissue independent of the BAT metabolic activation state. MRI is also associated with a lower cost and lack of ionizing radiation burden compared with ^{18}FDG-PET; as a result, brown adipose tissue imaging could be available to a larger patient population if performed by MRI.

Acknowledgements

The authors thank the staff of the Turku PET Center for their technical assistance.

Funding:

This study was conducted within the Finnish Centre of Excellence in Molecular Imaging in Cardiovascular and Metabolic Research, which is supported by the Academy of Finland,

University of Turku, Turku University Hospital and Åbo Akademi University. Additionally, RJHB received personal research grants from the Sigrid Juselius Foundation, the Instrumentarium Research Foundation, the Academy of Finland, the Paulo Foundation and the Finnish Medical Foundation.

Disclosure statement:

No potential conflicts of interest relevant to this article are reported.

Author contributions

All experiments were performed in the Turku PET Centre, University of Turku and Turku University Hospital, Turku, Finland.

Each author contributed significantly to the intellectual content of the article. MH, KAV, PN, RP and RJHB conceived of and designed the experiments. MH was responsible for coordinating the writing of the article and drafting the main text in cooperation with RJHB. KAV, PN, RP and JCH critically revised the article for important intellectual content. RJHB, MK, JS and VL outlined the physical principles and the calculations used in the DUAL SPIR MR imaging sequence and drafted the technical MR imaging section of the article. RJHB and VL conducted the actual imaging and MR data collection. MH analyzed and interpreted the MRI data and was responsible for post-processing of the images. TJG cared for the animals used in the studies, including their handling, anesthesia and ^{18}FDG-PET/CT examination, and analyzed and interpreted the ^{18}FDG-PET/CT data and drafted the corresponding part of the article. KAV dissected the animals, and JL performed histological examination of the dissected BAT samples and drafted the histology section of the manuscript. IL, an experienced biostatician, performed the statistical analysis and revised the applicable sections of the manuscript.

All of the authors approved the final version of the manuscript.

References:

1. Virtanen KA, Lidell ME, Orava J, et al. Functional brown adipose tissue in healthy adults. N Engl J Med 2009; 360:1518-1525.

2. Saito M, Okamatsu-Ogura Y, Matsushita M, et al. High incidence of metabolically active brown adipose tissue in healthy adult humans: effects of cold exposure and adiposity. Diabetes 2009; 58:1526-1531.

3. Huttunen P, Hirvonen J, Kinnula V. The occurrence of brown adipose tissue in outdoor workers. Eur J Appl Physiol Occup Physiol 1981; 46:339-345.

4. Cohade C, Mourtzikos KA, Wahl RL. "USA-Fat": prevalence is related to ambient outdoor temperature-evaluation with 18F-FDG PET/CT. J Nucl Med 2003; 44:1267-1270.

5. Kim S, Krynyckyi BR, Machac J, Kim CK. Temporal relation between temperature change and FDG uptake in brown adipose tissue. Eur J Nucl Med Mol Imaging 2008; 35:984-989.

6. van Marken Lichtenbelt WD, Vanhommerig JW, Smulders NM, et al. Cold-activated brown adipose tissue in healthy men. N Engl J Med 2009; 360:1500-1508.

7. Sethi JK, Vidal-Puig AJ. Targeting fat to prevent diabetes. Cell Metab 2007; 5:323-325.

8. Cinti S. The role of brown adipose tissue in human obesity. Nutr Metab Cardiovasc Dis 2006; 16:569-574.

9. Lin SC, Li P. CIDE-A, a novel link between brown adipose tissue and obesity. Trends Mol Med 2004; 10:434-439.

10. Claessens-van Ooijen AM, Westerterp KR, Wouters L, Schoffelen PF, van Steenhoven AA, van Marken Lichtenbelt WD. Heat production and body temperature during cooling and rewarming in overweight and lean men. Obesity (Silver Spring) 2006; 14:1914-1920.

11. Cypess AM, Lehman S, Williams G, et al. Identification and importance of brown adipose tissue in adult humans. N Engl J Med 2009; 360:1509-1517.

12. Ouellet V, Routhier-Labadie A, Bellemare W, et al. Outdoor Temperature, Age, Sex, Body Mass Index, and Diabetic Status Determine the Prevalence, Mass, and Glucose-Uptake Activity of 18F-FDG-Detected BAT in Humans. J Clin Endocrinol Metab 2010.

13. Pace L, Nicolai E, D'Amico D, et al. Determinants of Physiologic (18)F-FDG Uptake in Brown Adipose Tissue in Sequential PET/CT Examinations. Mol Imaging Biol 2010.

14. Nedergaard J, Bengtsson T, Cannon B. Unexpected evidence for active brown adipose tissue in adult humans. Am J Physiol Endocrinol Metab 2007; 293:E444-E452.

15. Dundamadappa SK, Shankar S, Danrad R, et al. Imaging of brown fat associated with adrenal pheochromocytoma. Acta Radiol 2007; 48:468-472.

16. Anderson SE, Schwab C, Stauffer E, Banic A, Steinbach LS. Hibernoma: imaging characteristics of a rare benign soft tissue tumor. Skeletal Radiol 2001; 30:590-595.

17. Baldi A, Santini M, Mellone P, et al. Mediastinal hibernoma: a case report. J Clin Pathol 2004; 57:993-994.

18. Furlong MA, Fanburg-Smith JC, Miettinen M. The morphologic spectrum of hibernoma: a clinicopathologic study of 170 cases. Am J Surg Pathol 2001; 25:809-814.

19. Seynaeve P, Mortelmans L, Kockx M, Van HM, Mathijs R. Case report 813: Hibernoma of the left thigh. Skeletal Radiol 1994; 23:137-138.

20. Osculati F, Leclercq F, Sbarbati A, Zancanaro C, Cinti S, Antonakis K. Morphological identification of brown adipose tissue by magnetic resonance imaging in the rat. Eur J Radiol 1989; 9:112-114.

21. Sbarbati A, Guerrini U, Marzola P, Asperio R, Osculati F. Chemical shift imaging at 4.7 tesla of brown adipose tissue. J Lipid Res 1997; 38:343-347.

22. Lunati E, Marzola P, Nicolato E, Fedrigo M, Villa M, Sbarbati A. In vivo quantitative lipidic map of brown adipose tissue by chemical shift imaging at 4.7 Tesla. J Lipid Res 1999; 40:1395-1400.

23. Chen YI, Cypess AM, Sass CA, Brownell AL, Jokivarsi KT, Kahn CR, Kwong KK. Anatomical and functional assessment of brown adipose tissue by magnetic resonance imaging. Obesity 2012; 20:1519-26.

24. Mosconi E, Fontanella M, Sima DM, Van Huffel S, Fiorini S, Sbarbati A, Marzola P. Investigation of adipose tissues in Zucker rats using in vivo and ex vivo magnetic resonance spectroscopy. J Lipid Res. 2011;52:330-6.

25. Hu HH, Hines CD, Smith DL Jr, Reeder SB. Variations in T(2)* and fat content of murine brown and white adipose tissues by chemical-shift MRI. Magn Reson Imaging 2012; 30:323-9.

26. Hu HH, Smith DL, Jr., Nayak KS, Goran MI, Nagy TR. Identification of brown adipose tissue in mice with fat-water IDEAL-MRI. J Magn Reson Imaging 2010; 31:1195-1202.

27. Hamilton G, Smith DL Jr, Bydder M, Nayak KS, Hu HH. MR properties of brown and white adipose tissues. J Magn Reson Imaging 2011; 34:468-73.

28. Poon CS, Szumowski J, Plewes DB, Ashby P, Henkelman RM. Fat/water quantitation and differential relaxation time measurement using chemical shift imaging technique. Magn Reson Imaging 1989; 7:369-382.

29. Tanaka S, Yoshiyama M, Imanishi Y, et al. Measuring visceral fat with water-selective suppression methods (SPIR, SPAIR) in patients with metabolic syndrome. Magn Reson Med Sci 2007; 6:171-175.

30. Hu HH, Nayak KS. Change in the proton T(1) of fat and water in mixture. Magn Reson Med 2010; 63:494-501.

31. Yokoo T, Bae WC, Hamilton G, et al. A quantitative approach to sequence and image weighting. J Comput Assist Tomogr 2010; 34:317-331.

Table 1: Brown adipose tissue (BAT) mass in all of the rats. The mass was measured by dissection, DUAL-SPIR MRI, conventional in- and out-of-phase MRI and ^{18}FDG-PET (N/A: data not available, I/A: insufficient activity observed in the PET data to allow for analysis). The results of the paired t-test comparisons of the BAT mass calculated using each individual technique versus the actual weight of BAT obtained through dissection are shown in the last row of the table.

	Weight of the rat (g)	**BAT in dissection (mg)**	**DUAL-SPIR MRI (mg)**	**In-and-out-of-phase MRI (mg)**	**^{18}FDG-PET/CT (mg)**
Rat 1	343	246	*N/A*	365	95
Rat 2	323	237	*N/A*	360	118
Rat 3	*N/A*	257	*N/A*	444	*N/A*
Rat 4	*N/A*	305	*N/A*	471	*N/A*
Rat 5	*N/A*	316	*N/A*	396	*N/A*
Rat 6	396	238	233	461	105
Rat 7	297	246	188	333	*I/A*
Rat 8	366	323	246	438	90
Rat 9	348	118	122	290	84
Rat 10	330	132	159	294	*I/A*
Rat 11	333	256	190	444	*I/A*
p-value	N/A	N/A	0.756	0.0026	0.0126

Figure legends

Figure 1, heading: **Interscapular brown adipose tissue (BAT) deposit in a rat.**

Figure 1, legend: Sagittal in-phase (1A), out-phase (1B) and DUAL-SPIR (1C) MR images depicting the interscapular brown adipose tissue (BAT) deposit in a rat. Figure 1C is a calculated subtraction image acquired by subtracting the out-of-phase images from the in-phase images, which were obtained following a spectral presaturation inversion recovery (SPIR) pulse. Interscapular BAT in rats consists of a central mass and a bilateral butterfly-shaped area (arrow). As can be observed, the DUAL-SPIR subtraction method makes the BAT tissue distinguishable from the surrounding white adipose tissue, in contrast to in- and out-of-phase imaging alone.

Figure 2, heading: **BAT activation in ^{18}FDG-PET/CT.**

Figure 2, legend: Examples of the ^{18}FDG-PET/CT 3D reconstruction of data obtained in animal nr. 9 (2A) showing the activation of brown adipose tissue (BAT) and in animal nr. 10 (2B), which had no clear BAT activation.

Figure 3, heading: **Image post-processing and fusion.**

Figure 3, legend: Calculated in- and out-of-phase subtraction DUAL-SPIR image of a rat interscapular BAT deposit acquired in the sagittal plane (3A) and ^{18}FDG-PET/CT images (3B) of the corresponding area. Figure 3C is a fusion image of these MR and ^{18}FDG-PET/CT images.

Figure 4, heading: **Correlation of the BAT mass acquired through dissection in rats in conjunction with DUAL-SPIR MRI, conventional in- and out-of-phase MRI and ^{18}FDG-PET/CT.**

Figure 4, legend: The autopsy results (black solid line) were most closely approximated by DUAL-SPIR MRI (SPIR, green dashed line), which appears to be superior to both conventional in- and out-of-phase imaging (non-SPIR, red dashed line) and ^{18}FDG-PET/CT (PET, blue dashed line).

Figure 5, heading: **Bland-Altman plots of the calculated BAT mass.**

Figure 5, legend: Bland-Altman plots of the calculated BAT mass based on MRI DUAL-SPIR images (5A), MRI conventional in- and out-of-phase images (5B) and ^{18}FDG-PET/CT images (5C) against the BAT mass measured in autopsy. DUAL SPIR MRI showed less bias and higher precision than 18FDG-PET/CT.

Figure 6, heading: **Human pilot cases.**

Figure 6, legend: Calculated in- and out-of-phase subtraction DUAL-SPIR images of the supraclavicular BAT deposits (arrow) in all 3 healthy human volunteers acquired in the coronal plane (6A) and ^{18}FDG-PET/CT images (6B) of the corresponding area in each subject. Figure 6C is a fusion image of these MR and ^{18}FDG-PET/CT images. The actual amount of brown adipose tissue mass estimated by each technique is stated in the Results section.

Figure 1:

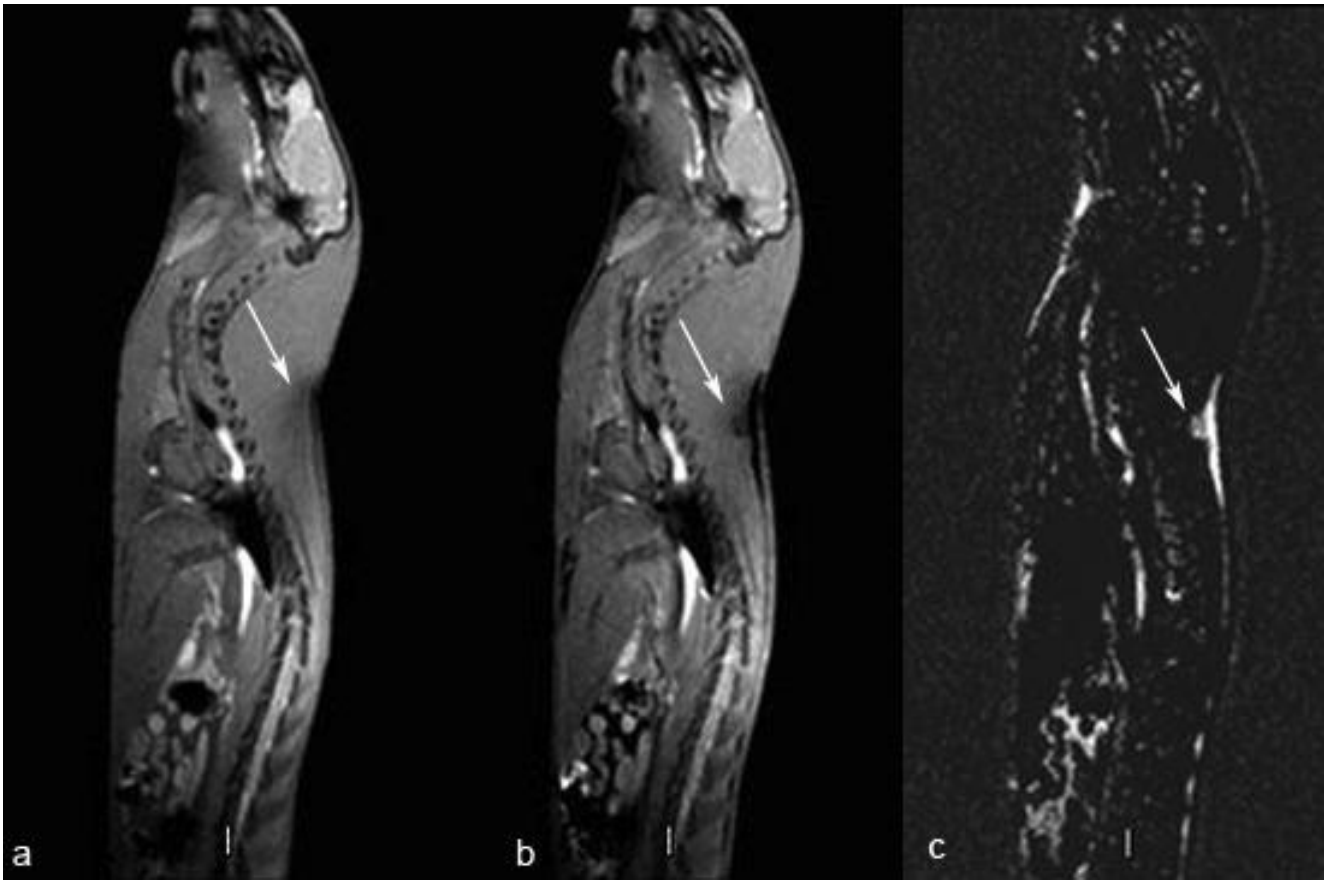

Figure 2:

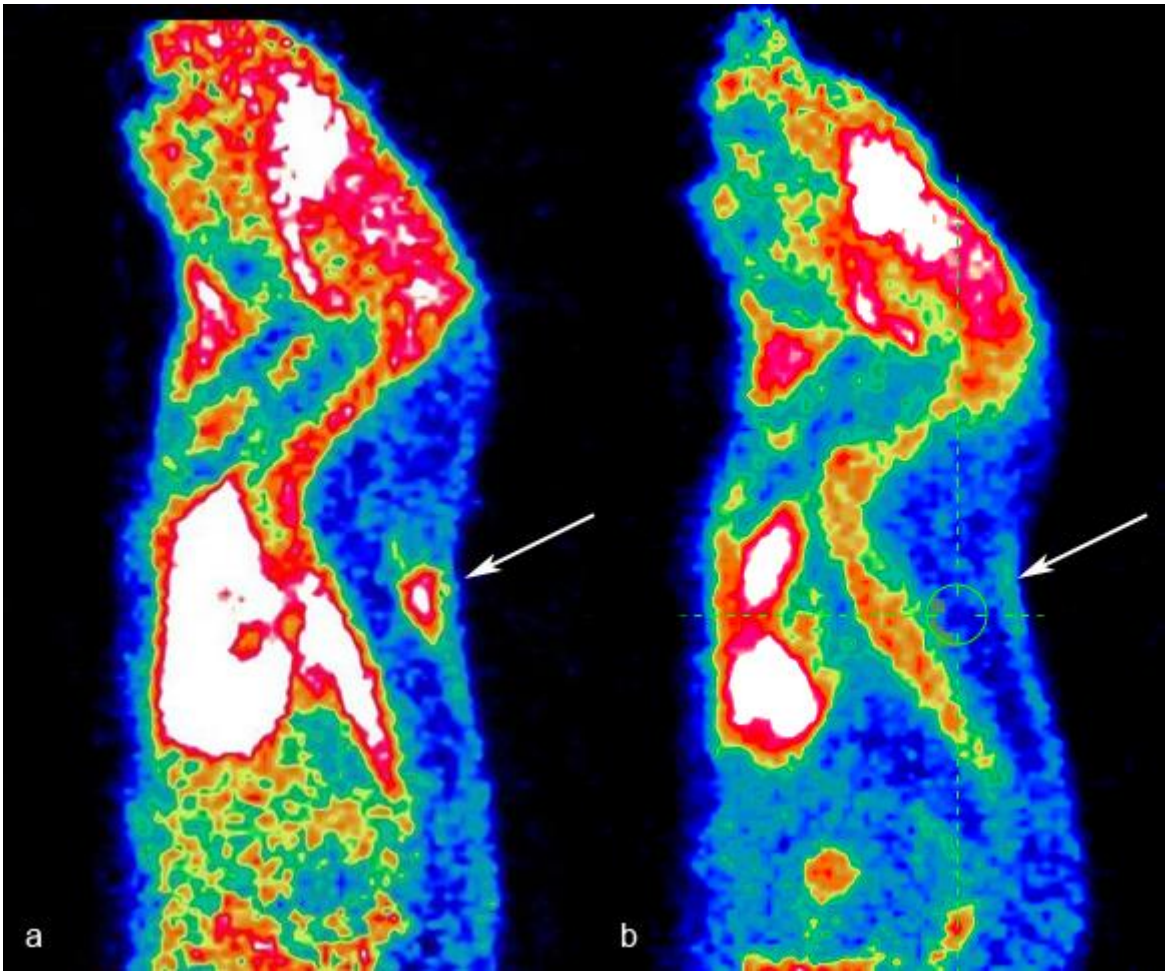

Figure 3:

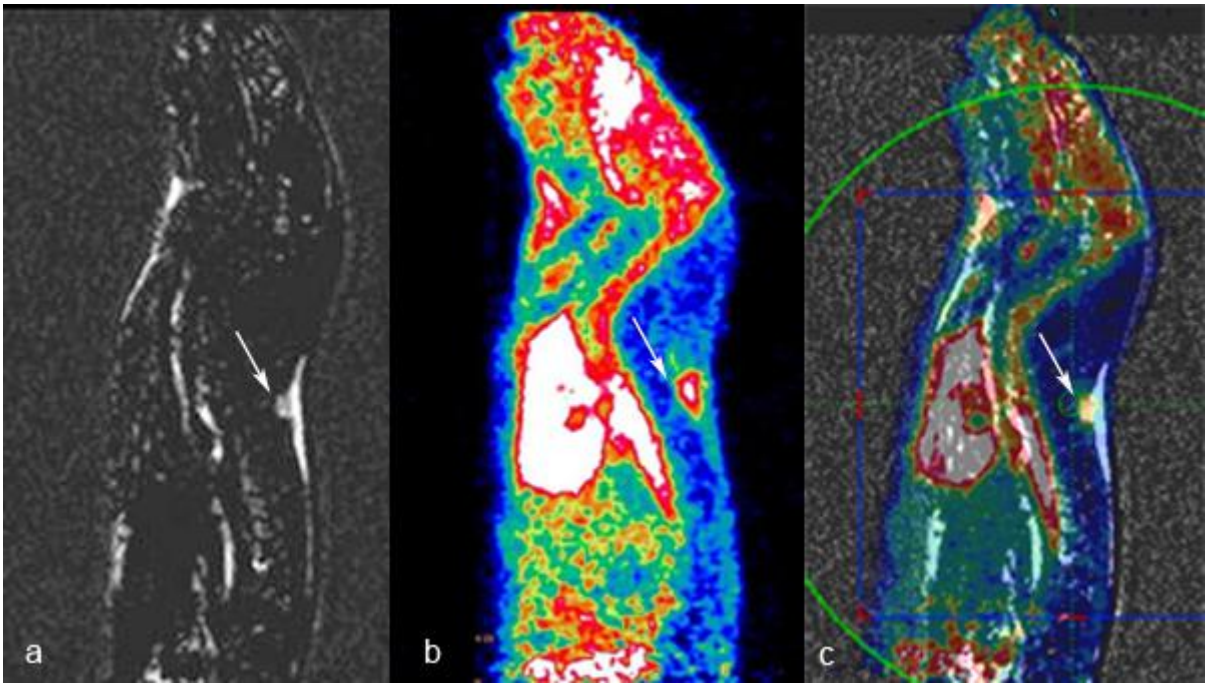

Figure 4:

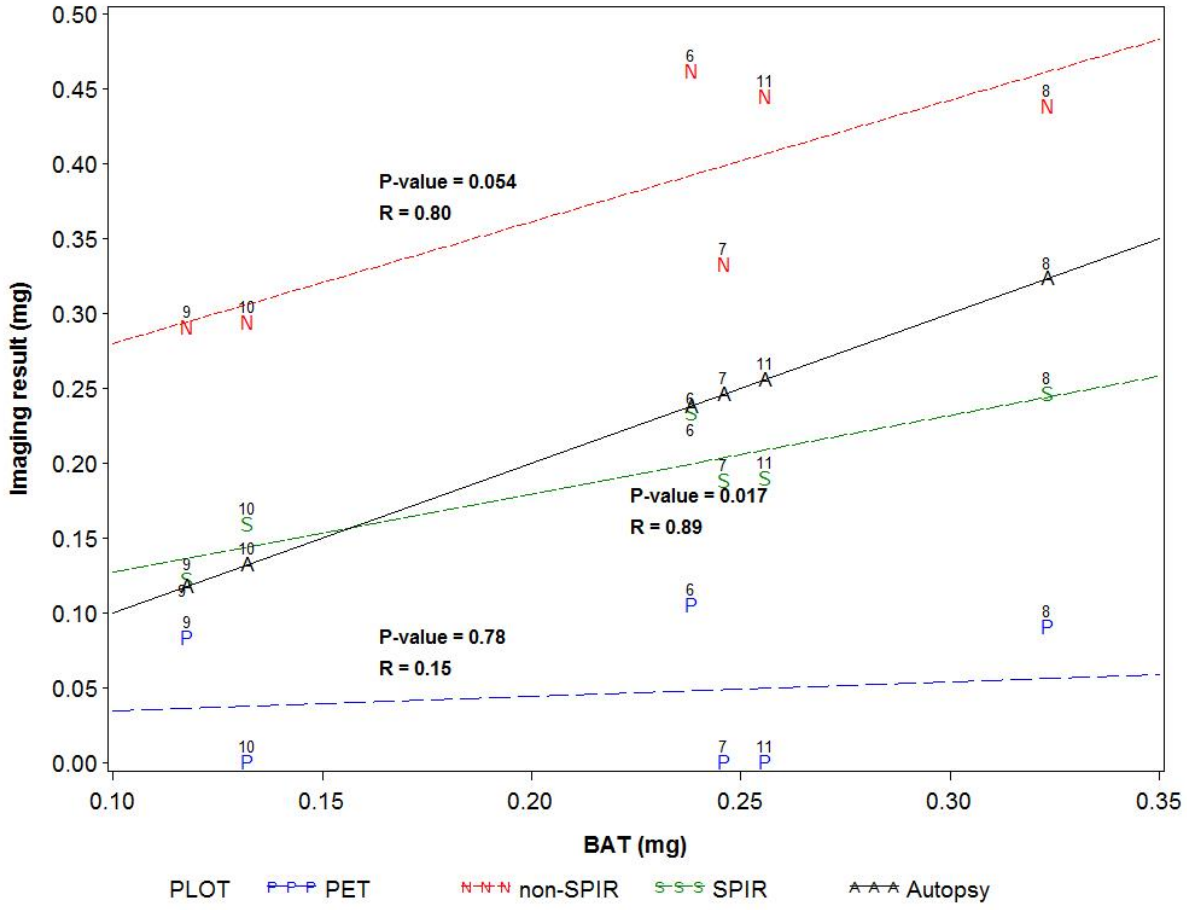
Imaging result (mg)
0.50
0.45
0.40
0.35
0.30
0.25
0.20
0.15
0.10
0.05
0.00
0.10
0.15
0.20
0.25
0.30
0.35
BAT (mg)
P-value = 0.054
R = 0.80
P-value = 0.017
R = 0.89
P-value = 0.78
R = 0.15
PLOT P P P PET N N N non-SPIR S S S SPIR A A A Autopsy

Figure 5a:

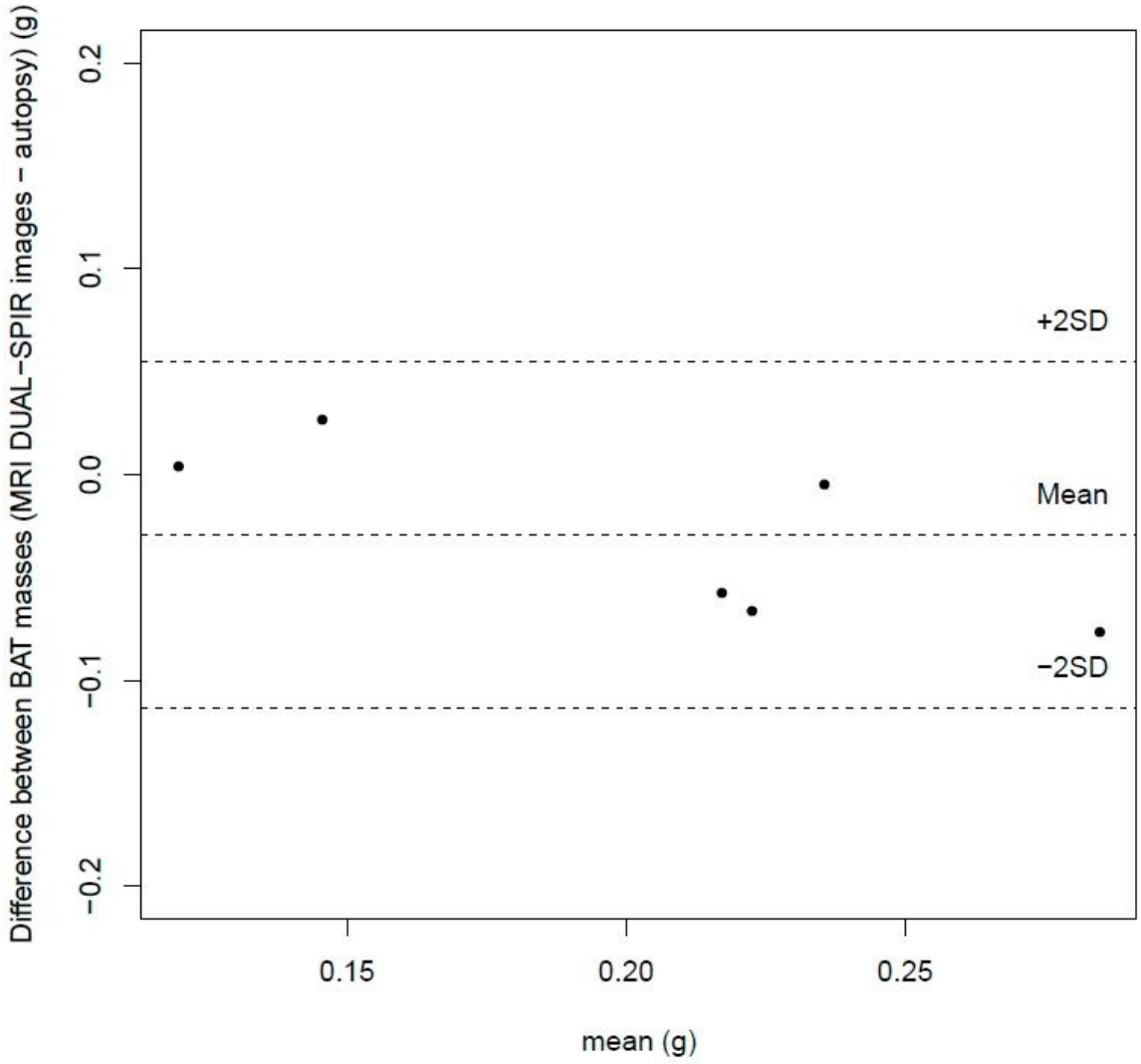
Difference between BAT masses (MRI DUAL−SPIR images − autopsy) (g)
0.2
0.1
0.0
−0.1
−0.2
+2SD
Mean
−2SD
0.15
0.20
0.25
mean (g)

Figure 5b:

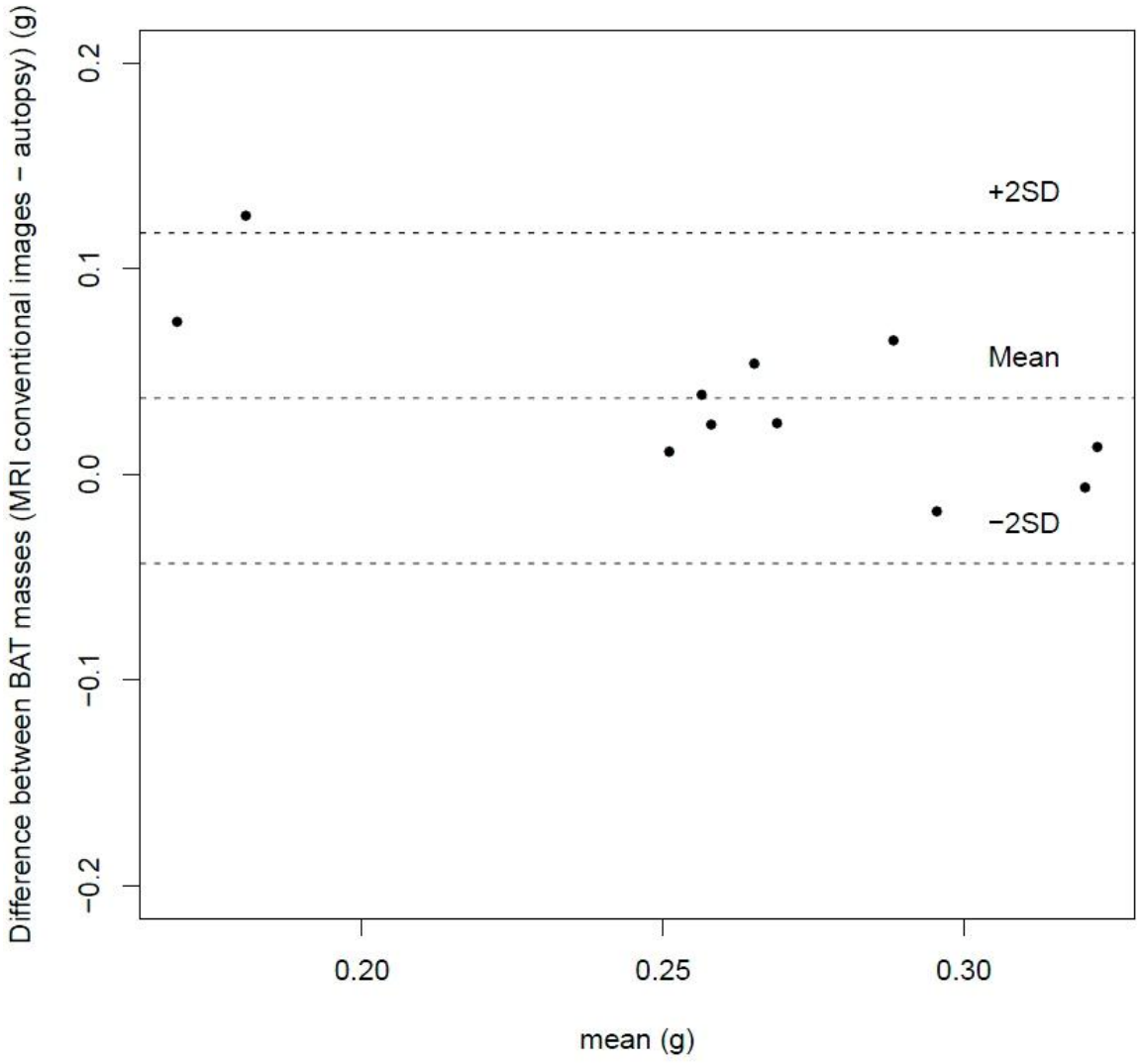
Difference between BAT masses (MRI conventional images − autopsy) (g)
0.2
0.1
0.0
−0.1
−0.2
+2SD
Mean
−2SD
0.20
0.25
0.30
mean (g)

Figure 5c:

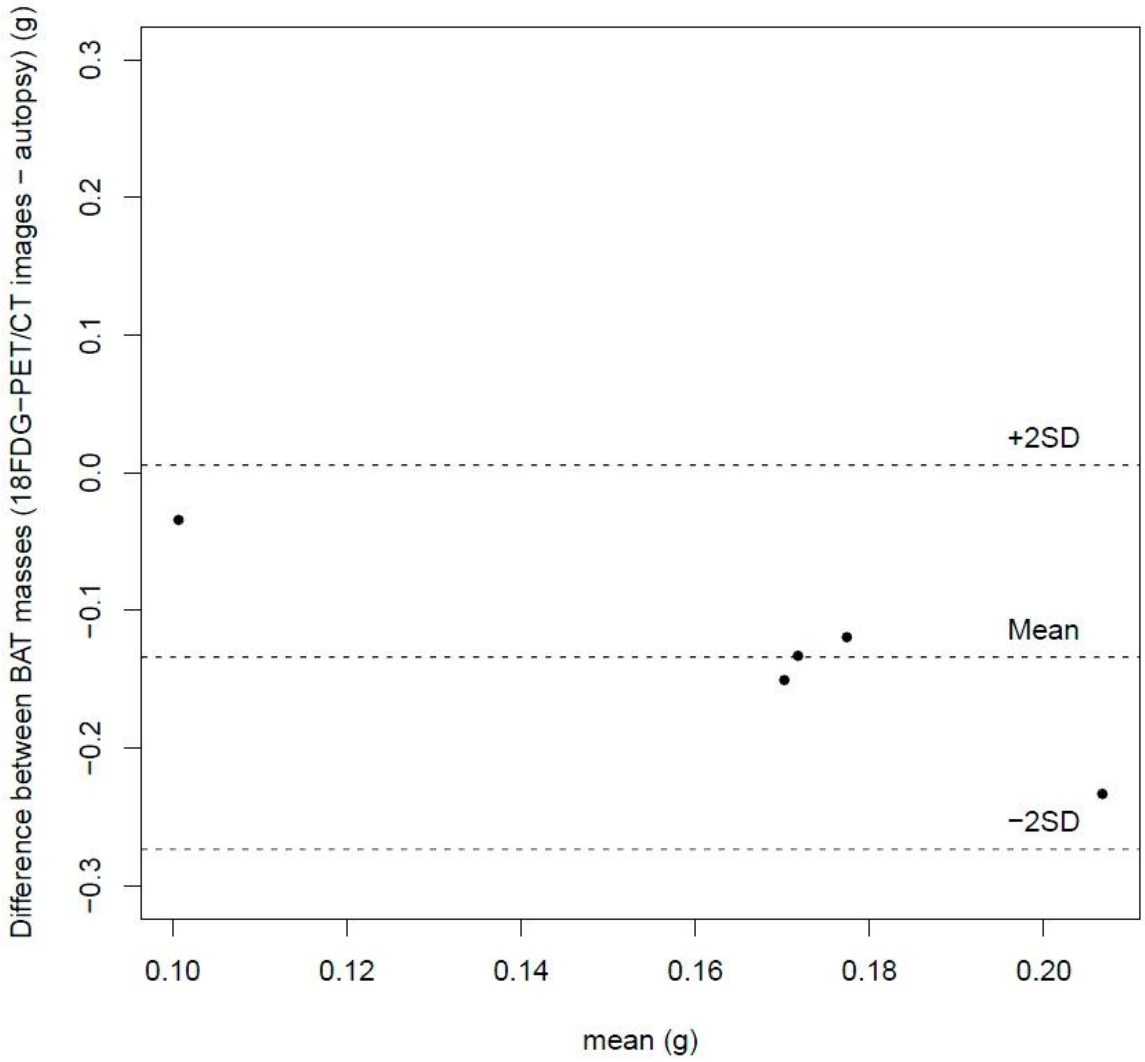
Difference between BAT masses (18FDG−PET/CT images − autopsy) (g)
0.3
0.2
0.1
0.0
−0.1
−0.2
−0.3
+2SD
Mean
−2SD
0.10
0.12
0.14
0.16
0.18
0.20
mean (g)

Figure 6: